Geospatial Model to Estimate Wind Energy Resource Potential in Remote Locations

Dr. Srikanth Narasimalu
Energy Research Institute @NTU (ERIAN)
1 Cleantech Loop, 06-04, Singapore 637141
Contact: nsrikanth@ntu.edu.sg

Ranjith Narasimhamurthy and Adithan Kannan
National Institute of Technology, Tiruchirappalli
Tamil Nadu, India. Pincode: 620015

***Abstract*—Remote locations in developing regions are experiencing one-fifth energy per capita and heavily depend on fossil fuels. To enhance energy security, all possible renewable energy resources should be exploited. The present state of the art technology demands deployment of wind mast and lidar based infrastructure which is laborious and costly and hence demands preliminary data for justification. This paper discusses a roughness estimation from a geospatial model from which the wind profile and the wind energy density can be estimated. Further spatial and temporal variation help perform macro level techno-economic estimates to identify best wind turbine placement sites and/or wind farm design sites which can be further confirmed by micro-level wind energy site assessment such as wind mast or lidar deployment complimented with computational fluid dynamics model of the terrain.**

***Index Terms*—wind energy, roughness, geospatial, renewable**

I. Introduction

According to the World Energy Forum, fossil-based oil, coal and gas reserves account for 80% of the primary energy supplied in the world [1]. The growing concerns related to the use of conventional forms of energy, primarily fossil-based, has shifted the focus towards renewables. Hence decision makers are keen to understand the renewable resource availability in their region to make fact based decisions. Concerns about energy security and resilience, economic growth in the face of rising energy prices, competitiveness, health costs and environmental degradation can be addressed by exploiting this renewable energy resources through appropriate resource assessment and adoption of renewable energy systems for the regional energy needs [2], [3].

Today, India ranks third in terms of energy consumption, followed by the People's Republic of China and the United States of America [1]. To be able to meet the energy requirements of such a fast-growing economy, a guaranteed supply of 3-4 times more than the energy consumed at present has to be met [2]. Wind energy plays a significant role in the Indian energy sector with a total installed capacity of 25.1 GW and accounts for 5.1% of the world's total wind energy production with a staggering 43 TWh of electricity produced [1]. Based on a prediction by using a logistic function, 99% of India's technical wind energy potential is expected to be achieved by the year 2030 [3].

978-1-5386-8136-7/18/$31.00 © 2018 IEEE

Wind power is a widely used renewable energy resource. Winds can be generated through complex mechanisms involving Coriolis forces, differential heating of the earth's surface, cooling effects of the oceans and polar ice caps, and physical effects of mountains and other obstacles. The kinetic energy of the wind has immense potential as a source of renewable energy in different parts of the world. About $3x10^{15}$ kWh or 0.2% of the solar energy reaching the earth is accounted for by the total annual kinetic energy of the atmosphere. However, only $30x10^{12}$ kWh/year or 35% of the current world total energy consumption can be used, according to theoretical estimates [4]. Wind turbines are used to harness wind energy. The power of wind blowing at 25.6 km/h is approximately 200 W/m^2 times the area swept by the wind turbine. About 36% of this power can be tapped as electricity [5].

Conventional methods to measure wind speed advocate setting up of cup or ultrasonic anemometers to measure wind speed. Anemometers set at different heights at different meteorological stations, must be adjusted to the same height before analysis. The standard height according to the World Meteorological Organization is 10 m above the ground level [6]. A point measurement is provided by the cup anemometer within a few centimeters [7]. Traditional meteorological towers are being replaced by more advantageous remote wind measurement devices such as sodar's and lidar's [8], [9]. These methods consume considerable time. Moreover, measurement of offshore wind speed is difficult to obtain through in-situ methods [10].

Technological advancements are accelerating at a fast pace. We are in an era where we can search the entire internet in less than a second. Thus, expectations of speed and retrieval of information have risen considerably. Efforts to reduce the time taken to solve complex problems has led to the evolution of many activity areas. Although in-situ observations play a critical role in calibrating and validating satellite observations in this satellite era, dense satellite sampling may reduce the role played by the in-situ observations in lowering random and sampling errors in blended analyses using in-situ and satellite observations [11].

II. LITERATURE REVIEW

A. Wind analysis

Wind Turbines capture the kinetic energy from wind and convert it into useful mechanical power. The useful power generated at the turbine is given by:

$$P = \frac{1}{2}\rho A v^3 C_p \tag{1}$$

where P is power produced in Watts, A is the area swept by the rotor in m^2, ρ is the density of air in kg/m^3, v is the velocity of incoming wind in m/s, and C_p is the power coefficient which is the ratio of power extracted by the turbine to that contained in the wind source. The density of air varies with temperature and elevation. Hence a correction factor must be accounted for while dealing with high altitudes. Since power produced depends on the cube of wind velocity, even a small change in velocity brings about significant changes in the power. Therefore, a clear understanding of wind velocity is of primary importance for initial site selection [12].

The influence of ground effects on wind speed is negligible at high altitudes, whereas, in the lowest atmospheric layers, the wind speeds are affected by ground friction factors. Wind shear in the first 400 feet is strictly site-dependent as it is a function of surface roughness, atmospheric stability, wind speed, height interval and varies with season and time of the day [13]–[16]. The regional wind speeds are also affected by topography and weather patterns. When the wind blows from flat terrain to a hill, the streamlines are compressed thereby causing it to speed up.

A wind profile is the representation of the variation of wind speed with height. The commonly used method is to estimate wind speeds at certain altitudes of a site using wind measuring techniques and extrapolate the readings to form a wind speed profile. The widely used laws are the Hellman's exponential law and the logarithmic profile law.

The Hellman's exponential law can be represented by:

$$\frac{v}{v_0} = \left(\frac{H}{H_0}\right)^{\alpha} \tag{2}$$

here v is the wind velocity at height H, v_0 is that velocity at height H_0 and α is the Hellman's exponent also known as friction coefficient. It varies with the topography of the site, atmospheric stability, time of the day and the height interval [17], [18]. Its a highly variable quantity, varying from 1/7 at the day to 1/2 during the night [19], [20]. The friction coefficient was also measured to range from 0.1 over smooth ground, water bodies to 0.4 in urban areas [15]. This profile is consistent with Weibull wind speed distribution which is very useful in Wind energy studies [21] though its validity is limited to 150-200m above ground level [17], [22].

The logarithmic profile law can be represented by:

$$\frac{v}{v_0} = \left(\frac{\ln H/Zo}{\ln H_0/Zo}\right) \tag{3}$$

in which v and v_0 are the wind speeds at heights H and H_0 respectively, and z_0 is aerodynamic roughness length in meters. This factor is characteristic to the type of land, shape, size and spacing of the roughness elements. z_0 typically varies from 0.0002 over water bodies to 1.5 in dense canopies and urban areas [23]. The roughness length for a homogenous terrain can be estimated by measurements at two different heights. Once we have obtained z_0 for a piece of land, the logarithmic formula can be used to calculate the speed at other heights [24].

It is common to extract predefined roughness values for different landscape types from tables, however, these values aren't accomplished and suitable for calculations. Given the velocities at specific heights, the aerodynamic roughness length can be estimated by the method mentioned below. Hence, a relation is devised between Hellman's exponent law and Logarithmic Law to calculate the roughness coefficient from at least two different heights over a reasonable period. The Hellman's exponent is first calculated for the two heights by using (2) and then equalizing (2) and (3), z_0 can be obtained from alpha by [22] :

$$z_o = exp\left[\frac{{H_0}^{\alpha}\ln H - H^{\alpha}\ln H_0}{{H_0}^{\alpha} - H^{\alpha}}\right] \tag{4}$$

The Weibull distribution function is used to study the distribution of wind velocities over a specified period. These family of curves provide an excellent fit to measured wind speed data. There are various methods to estimate the Weibull parameters. In this paper, the two parameter Maximum Likelihood Method has been chosen due to its flexibility and simplicity of estimation of parameters. This method provides a consistent approach for parameter estimation and has desirable mathematical and optimality properties [25]. It has also been demonstrated to be a more suitable computer-based method [26]. The shape parameter (k) and the scale parameter (c in m/s) can be calculated as follows:

$$k = \left[\frac{\sum_{i=1}^{n} v_i^k \ln v_i}{\sum_{i=1}^{n} v_i^k} - \frac{\sum_{i=1}^{n} \ln v_i}{n}\right]^{-1} \tag{5}$$

$$c = \left(\frac{1}{n}\sum_{i=1}^{n} v_i^k\right)^{\frac{1}{k}} \tag{6}$$

In which, v_i is the wind speed in time stage i and n is the number of non-zero wind speed data points. An initial value of 2 has been assumed for the shape parameter (k).

The relation between the Weibull parameters and the mean and most probable wind speed can be represented as follows:

$$\overline{v} = c\Gamma\left(1 + \frac{1}{k}\right) \tag{7}$$

$$V_{mp} = c\left(\frac{k-1}{k}\right)^{\frac{1}{k}} \tag{8}$$

Where $\overline{v}$ is the average speed, V_{mp} is the most probable wind speed, and Γ is the gamma function which is a continuous function defined for positive real numbers.

B. NDVI

Normalized Difference Vegetation Index is given by:

$$NDVI = \left[\frac{NIR - Red}{NIR + Red}\right] \tag{9}$$

where NIR and Red are radiances in Near Infra-Red and Red/Visible bands respectively.

The aerodynamic roughness length given by:

$$z_o = exp\Big(c_1 + c_2 NDVI\Big) \tag{10}$$

which is meant to describe the effects of roughness on surface drag as a function of NDVI for a particular crop. The coefficients depend on the vegetation type and phenology. However, the effect of a landscape structure on z_o is not described by this equation [27]. Accordingly, the present study focused to develop a general relationship between z_o and NDVI for any landscape structure under similar wind conditions.

Google earth Engine [28] is a cloud-based platform for planetary-scale-geospatial analysis. Earth Engine finds widespread use, covering topics like global forest change [29], global surface water change [30], crop yield estimation [31], rice paddy mapping [27], urban mapping [32], ood mapping [33], fire recovery [34] and malaria risk mapping [35]. Applications for analyzing species habitat ranges (Map of Life, 2016) [36], monitoring climate (Climate Engine, 2016) [37], and assessing land use change (Collect Earth, 2016) [38] have integrated Google Earth Engine into their applications.

Computation of z_o can be feasibly done only with the use of satellite data [39]. Traditionally, z_o can be calculated from measurements of wind profiles at different levels over the ground considering neutral atmospheric conditions [40]–[42]. According to long-term observations, for locations that have a similar type of coverage, modelers have assumed that momentum roughness is identical [43]. Aerodynamic roughness mainly depends on the geometric features and distributions of the roughness elements [44]. Estimation of z_o using an optical parameter called Normalized Difference Vegetation Index (NDVI) is a method that has been widely used [39], [45]–[47]. But all the efforts to establish a relationship between z_o and NDVI have been focused towards specific crop types.

For Wind Resource assessment and further siting, there is no established method for a quick estimation of (z_o) and further prediction of wind conditions [48] used a semi-empirical approach to determine z_o from satellite images. This paper aims to develop an empirical approach to draw a correlation between z_o derived from wind data and satellite data based NDVI for any terrain under consideration given similar wind conditions/climate type. Once a proper correlation has been established, then the satellite-based methodology could be effectively used to predict Roughness length without the necessity for in-situ wind data.

III. STUDY AREA

The present study focused its efforts for different locations in Tamil Nadu, India. Located in the extreme south of the subcontinent it is bound by the Indian Ocean to the east and south and by the states of Karnataka to the northwest, Kerala to the west and Andhra Pradesh to the north. With a total area of 130,058 km^2, Tamil Nadu is the 11th largest state in the country. The land is hilly and vegetation rich in the southern, western and north-western parts. It is the only state with the Western Ghats and Eastern Ghats meeting at the Nilgiri Hills. Much of the rain bearing clouds from the south-west monsoon is blocked from entering the state by the Western Ghats. While the eastern parts are fertile coastal plains, the northern parts are a mix of hill and plains. The south-central and central regions are arid plains.

Tamil Nadu, essentially tropical in climate, is heavily dependent on monsoon rains, thus prone to droughts in the absence of monsoons. The climate ranges from dry sub-humid to semi-arid [49]. The state has two distinct periods of rainfall:

- South-west monsoon with strong southwest winds - June to September
- North-east monsoon with dominant northeast winds - October to December

48% of the rainfall is through the North East monsoon while 32% is through the south-west monsoon. January to May is usually dry. The above factors play a crucial role in influencing the wind conditions of a location.

IV. METHODOLOGY

A. Calculation of roughness length

Acquiring long-term records of wind speed from a large number of well-exposed stations all over the region is an ideal method to predict the wind potential of an area [50]. Wind data was used to calculate the roughness length for various locations in Tamil Nadu. Wind Resource Assessment Data was collected from the Indian Meteorological Department, Pune for 13 locations. The TABLE I lists the coordinates of the data available, location wise. The mean and most probable wind speed was calculated for each location. The roughness length was for each of these wind speeds and have been tabulated as shown in TABLE II.

B. Determination of NDVI

Google Earth Engine was used for image acquisition, processing and analysis. A collection of images was acquired from the Landsat 8, an American earth observation satellite. The dataset available for analysis was calibrated for TOA (top of atmosphere) reflectance with orthorectified scenes only. The Red Band B4 (0.64 - 0.67 m) and the NIR Band B5 (0.85 - 0.88 m) have a high resolution of 30m. All the images available in the range Apr 11, 2013 - Apr 30, 2017, were stored in an image collection. The landsat 8 layers and NDVI layers have been shown for Dhanushkodi and Nallur in Fig1, Fig2, Fig3 and Fig 4. The image collection was composited using three different reducers. The image collection was composited using three different reducers:

- Mean reducer for compositing all the images in the collection to a single image representing the mean of the images.

- The greenest pixel composite was built using the quality mosaic method which uses a quality band as a per pixel ordering function.
- Median reducer was used for compositing all the images in the collection to a single image representing the median of the images.

TABLE I
LOCATION COORDINATES OF THE REGIONS OF INTEREST

LOCATION	LATITUDE	LONGITUDE
Subramaniyapuram	11.0639	78.6513
Ittarai	11.5952	77.0809
Kali	10.5758	77.6892
Karungal	10.7435	78.1380
Keeranipatti	10.0560	78.7127
Mellamandai	9.0798	78.2956
Nallur	11.38	77.1807
Udayalipatti	10.5837	78.8826
Viralimalai	10.6382	78.5283
Srivilliputhur	9.4730	77.7381
Sankarankovil	9.1592	77.5295
Dhanushkodi	9.1679	79.4289
Palaya Kundu	10.1411	77.7346

The region of interest was a 1km x 1km (approx.) square around the latitude and longitude coordinates under consideration. NDVI value was calculated for each pixel in the region of interest. Then, a mean reducer was used to return the arithmetic mean of all the individual pixel NDVI values. This procedure was repeated for all the latitudes and longitude coordinates under consideration, and the results have been indicated in TABLE III.

V. RESULTS AND DISCUSSION

The roughness lengths calculated using the values of mean velocity and most probable velocities at two different heights have been tabulated in TABLE II. The values have been calculated for two different pairs of heights. One set of roughness length values have been calculated with values from 10 m and 50 m and other set has been calculated with values from 10 m and 80 m.

It can be observed that the roughness length values calculated from Mean velocities at 10m and 50m are within the acceptable range of values for roughness lengths as shown in TABLE V. All the calculations are based on experimental findings. Any error in the calculated value could be due to external influence or failure in the sensor. One obvious outlier in the z_o calculated from the mean velocities at 10 m and 50 m is for the area of Keeranipatti. The value of 1.5409 is higher than usual standards. An interesting observation is an extremely low value for Dhanushkodi. This is mainly due to an influence of the surrounding sea and its effects. The value of z_o calculated from the mean velocities at 10 m and 80 m is also within the acceptable range except for the area of Keeranipatti. It has an extremely high value of 1.6147.

Roughness length values evaluated from the most probable velocities for the heights 10 m and 50 m as well as for the heights 10m and 80 m show observable deviations from the accepted range of values. Based on the values in TABLE II it

TABLE II
ROUGHNESS LENGTH VALUES FOR THE DIFFERENT LOCATIONS OBTAINED FROM THE DIFFERENT MEAN AND MOST PROBABLE WIND SPEED FOR TWO DIFFERENT PAIRS OF HEIGHTS - 10M & 50M; 10M & 80M

LOCATION	MEAN z_0[10-50]	MPW z_0[10-50]	MEAN z_0[10-80]	MPW z_0[10-80]
Subramaniyapuram	0.106	0.3843	0.1096	0.2975
Ittarai	0.5912	1.8533	0.3956	1.2676
Kali	0.3150	1.4668	0.3823	1.7247
Karungal	0.2432	0.5914	0.2834	0.5335
Keeranipatti	1.5409	2.4336	1.6147	2.4691
Mellamandai	0.4274	1.1912	0.2831	0.9496
Nallur	0.4748	0.8204	0.5113	0.7898
Udayalipatti	0.5533	1.1246	0.5195	0.6999
Viralimalai	0.1564	0.2120	0.2488	0.5963
Srivilliputhur	0.0800	0.2262	0.1630	0.3540
Sankarankovil	0.4651	0.8349	0.4343	0.7824
Dhanushkodi	1.27e-9	1.18e-14	4.96e-22	5.29e-12
Palaya Kundu	0.0221	0.0007	0.282	0.0843

TABLE III
NDVI VALUES OBTAINED USING THE THREE DIFFERENT REDUCERS

LOCATION	NDVI [Median Filter]	NDVI [Mean Filter]	NDVI [Greenest Pixel Composite]
Subramaniyapuram	0.2989	0.1878	0.4989
Ittarai	0.5295	0.2444	0.7437
Kali	0.2603	0.2080	0.5759
Karungal	0.2448	0.1997	0.6161
Keeranipatti	0.3078	0.2300	0.4778
Mellamandai	0.2779	0.1999	0.6221
Nallur	0.3037	0.2267	0.6036
Udayalipatti	0.3040	0.2170	0.5343
Viralimalai	0.2665	0.2262	0.5033
Srivilliputhur	0.2754	0.2159	0.5305
Sankarankovil	0.2363	0.1812	0.5094
Dhanushkodi	-0.0609	-0.0153	0.1035
Palaya Kundu	0.2677	0.2384	0.5677

Fig. 1. NDVI Layer- Dhanushkodi

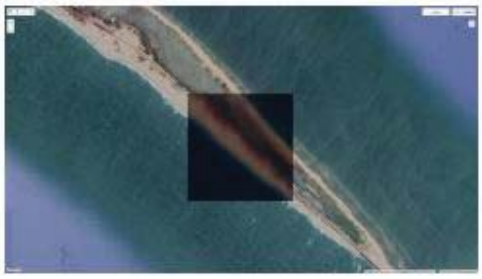

Fig. 2. Landsat 8 - Dhanushkodi

Fig. 3. NDVI Layer- Nallur

Fig. 4. Landsat 8- Nallur

can be inferred that roughness length must not be calculated from the most probable velocities. Only the mean velocities provide an acceptable value of roughness length.

The aim was to compare the calculated roughness length values with the NDVI values obtained from the different methods of image processing and investigate the existence of a correlation. Scatter plots were drawn to visualize the strength of the relationship between the mean z_o for the two different pairs of heights and the NDVI from the three methods of processing. The results have been tabulated in TABLE IV. The observable outliers were removed before plotting the graph. A simple linear fit regression line was drawn after eliminating the outliers. The coefficient of determination, a good measure to compare the strength of a correlation was also found.

From TABLE IV it can be observed that the highest coefficient of determination is for the plot between z_o calculated from the mean values of velocity for the heights 10 m and 80 m and the NDVI determined by using the greenest pixel composite. The value is found to be 0.4098. The coefficient of determination was least for the plot between the roughness length values calculated from the pair of 10 m and 50 m pair and the NDVI determined from applying the mean Filter. This value is 0.1736. The coefficient of determination can be improved if more values are closer to the linear fit line. The sample space of this data has only 13 points. It is not feasible to draw any inferences from such a small dataset. Valid inferences can be made only if the dataset is more populated. Such comparison would be more feasible if more data from other locations with a similar wind climate is obtained. There is an emphasis on similar wind climate since wind conditions are majorly influenced by the climate of the area.

The proposed methodology is capable of assisting studies that have been conducted in the past. The effects of ocean surface waves and atmospheric boundary layer on the storm track and intensity of the cyclones [51] were investigated using numerical simulations. The roughness length obtained from the present method facilitates the study of the atmospheric boundary layer, thereby simplifying ocean surface studies. Also, variance characteristics of upper-air winds obtained using radiosonde observations [52] can be studied in more detail with a better understanding of the atmospheric boundary layer.

Power generation is an avenue that requires a lot of attention, especially in energy intensive countries [53]. Energy production capacity of wind turbines can be derived from wind profile extrapolations. This can be used to perform wind turbine sizing according to the regional wind climate, leading to site-turbine matching. The results of the study can also be used to optimize the wind farm layout.

VI. CONCLUSION

The present study has provided a cost effective Geospatial based data analysis to estimate the wind roughness prediction of a remote site. This helps to estimate a wind velocity distribution of a broad region and thereby the wind energy density maps can be generated. Such data helps identify the best windy locations to further perform micro-sitting to choose the wind turbine placement and/or design a suitable wind farm in the given terrain. Further using the wind roughness z_o value, the wind shear phenomena with altitude can be estimated and the appropriate minimal height with stable wind condition can be estimated.

TABLE IV
RESULTS OBTAINED FROM THE SCATTER PLOTS

PLOT	EQUATION	R-SQUARED
Mean Z0[10-50] vs NDVI [Median Filter]	y=0.985x+0.022	0.3575
Mean Z0[10-50] vs NDVI [Mean Filter]	y=1.2906x+0.0356	0.1736
Mean Z0[10-50] vs NDVI [Greenest Pixel Composite]	y=0.8187x-0.151	0.3423
Mean Z0[10-80] vs NDVI [Median Filter]	y=0.702x+0.1136	0.3255
Mean Z0[10-80] vs NDVI [Mean Filter]	y=1.4362x+0.0222	0.3888
Mean Z0[10-80] vs NDVI [Greenest Pixel Composite]	y=0.666x-0.0546	0.4098

TABLE V
ROUGHNESS LENGTH CLASSIFICATION ACCORDING TO TERRAIN SURFACE CHARACTERISTICS[17]

z_0[m]	Terrain Surface Characteristics (land use)
1.5	Sparse forest
1	City
0.8	Dense forest
0.5	Suburbs
0.4	Shelter belts
0.2	Many trees and/or bushes
0.1	Farmland with closed appearance
0.05	Farmland with open appearance
0.03	Farmland with very few buildings/trees
0.02	Airport areas with some buildings and trees
0.01	Airport runway areas
0.008	Mown grass
0.005	Bare soil (smooth)
0.001	Snow surface (smooth)
0.0003	Sand surface (smooth)
0.0002	Water areas (lakes, fjords, open sea)

ACKNOWLEDGMENT

The authors would like to thank Energy Research Institute@ NTU for supporting this research to promote the diffusion of wind energy technologies towards remote regions energy security in developing countries.

REFERENCES

[1] IEA International Energy Agency. Key world energy statistics. https://www.iea.org/publications/freepublications/publication/KeyWorld2017.pdf. Accessed on 2018-07-09.

[2] Ashwani Kumar, Kapil Kumar, Naresh Kaushik, Satyawati Sharma, and Saroj Mishra. Renewable energy in india: current status and future potentials. *Renewable and Sustainable Energy Reviews*, 14(8):2434–2442, 2010.

[3] M Carolin Mabel and E Fernandez. Growth and future trends of wind energy in india. *Renewable and Sustainable Energy Reviews*, 12(6):1745–1757, 2008.

[4] Leslie Clifford Wilbur. Handbook of energy systems engineering: Production and utilization. 1985.

[5] TV Ramachandra, DK Subramanian, and NV Joshi. Wind energy potential assessment in uttara kannada district of karnataka, india. *Renewable Energy*, 10(4):585–611, 1997.

[6] World Meteorological Organisation. Guide to meteorological instrument and observing practices. https://library.wmo.int/pmb$_ged/wmo_{8e}n-2012.pdf$.

[7] Shafiqur Rehman, Mohammed A Mohandes, and Luai M Alhems. Wind speed and power characteristics using lidar anemometer based measurements. *Sustainable Energy Technologies and Assessments*, 27:46–62, 2018.

[8] SG Bradley, Ioannis Antoniou, S Von Hunerbein, Detlef Kindler, HE Jorgensen, M De Noord, et al. Sodar calibration for wind energy applications, final reporting on wp3, eu wise project nne5-2001-297. 2005.

[9] A Albers. Evaluation of zephir. *Deutsche WindGuard Consulting GmbH Report, Germany*, 2006.

[10] Huai-Min Zhang, John J Bates, and Richard W Reynolds. Assessment of composite global sampling: Sea surface wind speed. *Geophysical Research Letters*, 33(17), 2006.

[11] Huai-Min Zhang, Richard W Reynolds, and Thomas M Smith. Adequacy of the in situ observing system in the satellite era for climate sst. *Journal of Atmospheric and Oceanic Technology*, 23(1):107–120, 2006.

[12] Gilbert M Masters. *Renewable and efficient electric power systems*. John Wiley & Sons, 2013.

[13] JO Counihan. Adiabatic atmospheric boundary layers: a review and analysis of data from the period 1880–1972. *Atmospheric Environment (1967)*, 9(10):871–905, 1975.

[14] Carl Gerald Justus. Winds and wind system performance. *Research supported by the National Science Foundation and Energy Research and Development Administration. Philadelphia, Pa., Franklin Institute Press, 1978. 120 p.*, 1978.

[15] John S Irwin. A theoretical variation of the wind profile power-law exponent as a function of surface roughness and stability. *Atmospheric Environment (1967)*, 13(1):191–194, 1979.

[16] David A Spera. *Introduction to modern wind turbines*. ASME Press: New York, 1994.

[17] F Bañuelos-Ruedas, C Angeles-Camacho, and S Rios-Marcuello. Analysis and validation of the methodology used in the extrapolation of wind speed data at different heights. *Renewable and Sustainable Energy Reviews*, 14(8):2383–2391, 2010.

[18] Giovanni Gualtieri and Sauro Secci. Wind shear coefficients, roughness length and energy yield over coastal locations in southern italy. *Renewable Energy*, 36(3):1081–1094, 2011.

[19] D Camblong. *Minimización de impacto de las perturbaciones de origen eólico en la generación por aeroturbinas de velocidad variable*. PhD thesis, PhD Thesis. Mondragón Unibertsitatea, Spain, 2003.

[20] DA Spera and TR Richards. Modified power law equations for vertical wind profiles. 1979.

[21] CG Justus and Amir Mikhail. Height variation of wind speed and wind distributions statistics. *Geophysical Research Letters*, 3(5):261–264, 1976.

[22] Károly Tar. Some statistical characteristics of monthly average wind speed at various heights. *Renewable and Sustainable Energy Reviews*, 12(6):1712–1724, 2008.

[23] Gustavo Montero, Eduardo Rodríguez, Albert Oliver, Javier Calvo, José M Escobar, and Rafael Montenegro. Optimisation technique for improving wind downscaling results by estimating roughness parameters. *Journal of Wind Engineering and Industrial Aerodynamics*, 174:411–423, 2018.

[24] MA Borja Díaz, R González-Galarza, F Mejía-Neri, JM Huacuz-Villamar, R Saldaña-Flores, and MC Medrano-Vaca. Estado del arte y tendencias de la tecnología eoloeléctrica. *PUE-UNAM, Instituto de Investigaciones Eléctricas, México*, 1998.

[25] Jose A Carta, Penelope Ramirez, and Sergio Velazquez. A review of wind speed probability distributions used in wind energy analysis:

Case studies in the canary islands. *Renewable and Sustainable Energy Reviews*, 13(5):933–955, 2009.
[26] JV Seguro and TW Lambert. Modern estimation of the parameters of the weibull wind speed distribution for wind energy analysis. *Journal of Wind Engineering and Industrial Aerodynamics*, 85(1):75–84, 2000.
[27] Jinwei Dong, Xiangming Xiao, Michael A Menarguez, Geli Zhang, Yuanwei Qin, David Thau, Chandrashekhar Biradar, and Berrien Moore III. Mapping paddy rice planting area in northeastern asia with landsat 8 images, phenology-based algorithm and google earth engine. *Remote sensing of environment*, 185:142–154, 2016.
[28] Noel Gorelick, Matt Hancher, Mike Dixon, Simon Ilyushchenko, David Thau, and Rebecca Moore. Google earth engine: Planetary-scale geospatial analysis for everyone. *Remote Sensing of Environment*, 202:18–27, 2017.
[29] Matthew C Hansen, Peter V Potapov, Rebecca Moore, Matt Hancher, SAA Turubanova, Alexandra Tyukavina, David Thau, SV Stehman, SJ Goetz, TR Loveland, et al. High-resolution global maps of 21st-century forest cover change. *science*, 342(6160):850–853, 2013.
[30] Jean-François Pekel, Andrew Cottam, Noel Gorelick, and Alan S Belward. High-resolution mapping of global surface water and its long-term changes. *Nature*, 540(7633):418, 2016.
[31] David B Lobell, David Thau, Christopher Seifert, Eric Engle, and Bertis Little. A scalable satellite-based crop yield mapper. *Remote Sensing of Environment*, 164:324–333, 2015.
[32] Qingling Zhang, Bin Li, David Thau, and Rebecca Moore. Building a better urban picture: Combining day and night remote sensing imagery. *Remote Sensing*, 7(9):11887–11913, 2015.
[33] Brian Coltin, Scott McMichael, Trey Smith, and Terrence Fong. Automatic boosted flood mapping from satellite data. *International Journal of Remote Sensing*, 37(5):993–1015, 2016.
[34] Christopher E Soulard, Christine M Albano, Miguel L Villarreal, and Jessica J Walker. Continuous 1985–2012 landsat monitoring to assess fire effects on meadows in yosemite national park, california. *Remote Sensing*, 8(5):371, 2016.
[35] Hugh JW Sturrock, Justin M Cohen, Petr Keil, Andrew J Tatem, Arnaud Le Menach, Nyasatu E Ntshalintshali, Michelle S Hsiang, and Roland D Gosling. Fine-scale malaria risk mapping from routine aggregated case data. *Malaria journal*, 13(1):421, 2014.
[36] Map of life,2016. http://www.mol.org. Accessed on 2018-07-10.
[37] University of Idaho Desert Research Institute. Climate engine, 2016. http://climateengine.org, 2016. Accessed on 2018-07-10.
[38] United Nations Food and Agricultu re Organization. Collect earth, 2016. http://www.openforis.org/tools/collect-earth.html. Accessed on 2018-07-10.
[39] RK Gupta, TS Prasad, and D Vijayan. Estimation of roughness length and sensible heat flux from wifs and noaa avhrr data. *Advances in Space Research*, 29(1):33–38, 2002.
[40] Tmuya Hryama, Michiaki Sugita, and Kazuo Kotoda. Regional roughness parameters and momentum fluxes over a complex area. *Journal of Applied Meteorology*, 35(12):2179–2190, 1996.
[41] Béatrice Marticorena, Mouldi Kardous, Gilles Bergametti, Yann Callot, Patrick Chazette, Houcine Khatteli, Le Hégarat-Mascle, Michel Maille, Jean-Louis Rajot, Daniel Vidal-Madjar, et al. Surface and aerodynamic roughness in arid and semiarid areas and their relation to radar backscatter coefficient. *Journal of Geophysical Research: Earth Surface*, 111(F3), 2006.
[42] J.L Monteith. *In Principles of Environmental Physics*, pages 190–215. Edward Arnold: London, UK, 1973.
[43] Fei Chen, Kenneth Mitchell, John Schaake, Yongkang Xue, Hua-Lu Pan, Victor Koren, Qing Yun Duan, Michael Ek, and Alan Betts. Modeling of land surface evaporation by four schemes and comparison with fife observations. *Journal of Geophysical Research: Atmospheres*, 101(D3):7251–7268, 1996.
[44] Kyle D Maurer, Brady S Hardiman, Christoph S Vogel, and Gil Bohrer. Canopy-structure effects on surface roughness parameters: Observations in a great lakes mixed-deciduous forest. *Agricultural and forest meteorology*, 177:24–34, 2013.
[45] KJ Schaudt and RE Dickinson. An approach to deriving roughness length and zero-plane displacement height from satellite data, prototyped with boreas data. *Agricultural and Forest Meteorology*, 104(2):143–155, 2000.
[46] Jia Li, Wang Jiemin, and Massimo Menenti. Estimation of area roughness length for momentum using remote sensing data and measurements in field. *Scientia Atmospherica Sinica*, 5:013, 1999.
[47] J Zhang, JP Huang, and Q Zhang. Retrieval of aerodynamic roughness length character over sparse vegetation region. *Acta Ecol Sin*, 30:2819–2827, 2010.
[48] Noram I Ramli, M Idris Ali, M Syamsyul H Saad, and TA Majid. Estimation of the roughness length (zo) in malaysia using satellite image. *Wind Engineering*, 2009.
[49] BMK Raju, KV Rao, B Venkateswarlu, AVMS Rao, CA Rama Rao, VUM Rao, B Bapuji Rao, N Ravi Kumar, R Dhakar, N Swapna, et al. Revisiting climatic classification in india: a district-level analysis. *Current Science*, pages 492–495, 2013.
[50] TV Ramachandra and BV Shruthi. Wind energy potential mapping in karnataka, india, using gis. *Energy conversion and management*, 46(9-10):1561–1578, 2005.
[51] Nikhil Garg, Eddie Yin Kwee Ng, and Srikanth Narasimalu. The effects of sea spray and atmosphere–wave coupling on air–sea exchange during a tropical cyclone. *Atmospheric Chemistry and Physics*, 18(8):6001, 2018.
[52] Jing-Jin Tieo, Tieh-Yong Koh, Martin Skote, and Narasimalu Srikanth. Variance characteristics of tropical radiosonde winds using a vector-tensor method. *Energies*, 11(1):137, 2018.
[53] BR Karthikeya, Prabal S Negi, and N Srikanth. Wind resource assessment for urban renewable energy application in singapore. *Renewable Energy*, 87:403–414, 2016.